Proceedings of the Combustion Institute, Volume 28, 2000/pp. 2843–2849

FLAME SPREAD ALONG FREE EDGES OF THERMALLY THIN SAMPLES IN MICROGRAVITY

W. E. MELL,[1] S. L. OLSON[2] AND T. KASHIWAGI[3]
[1]*Chemical and Fuels Engineering Department*
University of Utah
Salt Lake City, UT 84112, USA
[2]*Microgravity Combustion Science Branch*
NASA Glenn Research Center
Cleveland, OH 44135, USA
[3]*Building and Fire Research Laboratory*
National Institute of Standards and Technology
Gaithersburg, MD 20899, USA

The effects of imposed flow velocity on flame spread along open edges of a thermally thin cellulosic sample in microgravity were studied experimentally and theoretically. In this study, the sample was ignited locally at the middle of the 4 cm wide sample, and subsequent flame spread reached both open edges of the sample along the direction of the flow. The following flame behaviors were observed in the experiments and predicted by the numerical calculation, in order of increased imposed flow velocity: (1) ignition but subsequent flame spread was not attained, (2) flame spread upstream (opposed mode) without any downstream flame, and (3) the upstream flame and two separate downstream flames traveled along the two open edges (concurrent mode). Generally, the upstream and downstream edge flame spread rates were faster than the central flame spread rate for an imposed flow velocity of up to 5 cm/s. This was due to greater oxygen supply from the outer free stream to the edge flames and more efficient heat transfer from the edge flames to the sample surface than the central flames. For the upstream edge flame, flame spread rate was nearly independent of, or decreased gradually with, the imposed flow velocity. The spread rate of the downstream edge, however, increased significantly with the imposed flow velocity.

Introduction

Fire safety precautions will be especially vital for the longer duration and increasingly complex space missions in the future International Space Station and the planned manned flight mission to Mars (three years). For this reason, many flame spread experiments over combustible solid surfaces have been conducted in microgravity environments: for example, over a thermally thin cellulosic sample with external flows [1,2]; at various ambient pressures in a quiescent environment [3,4]; in a three-dimensional spread pattern from a localized spot ignition [5]; and over a thermally thick polymethylmethacrylate (PMMA) sample in quiescent, high oxygen concentration environments [6,7]. All these experiments were conducted over the center part of the sample to avoid the effects of the sample edges as much as possible. However, limited published studies on flame spread along thin sample edges in normal gravity have shown that flame spread rate along free edges tends to be faster than that along the center of the sample [8,9]. Since faster flame spread rate means more rapid fire growth, measurements of spread rates along free edges in microgravity are needed. A slow external flow, which simulates ventilation flow in a spacecraft and the Space Station, has significant effects on flame spread in microgravity [1,2,10]. Thus, the focus of this paper is to determine the effects of a slow imposed flow on both flame spread behavior and spread rate along free edges in microgravity and to understand their controlling mechanisms.

Flight Hardware

Flame spread experiments were performed in the Space Shuttle during the STS-75 USMP-3 mission. The Radiative Ignition and Transition to Spread Investigation (RITSI) flight hardware was used within the Shuttle middeck Glovebox facility and consisted of a small duct test section (8.5 cm wide $\times$ 9.5 cm high $\times$ 17.1 cm long) through which fan-drawn air flow passed smoothly at speeds from 0 to 6.5 cm/s in the lengthwise direction. The estimate of uncertainty of the flow velocity was ± 0.5 cm/s based on the calibration data and the accuracy of a low-velocity hot wire. Samples were 4 cm wide by 10 cm long sheets of ashless filter paper (area density of 0.0077

Report Documentation Page

Form Approved
OMB No. 0704-0188

1. REPORT DATE	2. REPORT TYPE	3. DATES COVERED
04 AUG 2000	**N/A**	**-**

4. TITLE AND SUBTITLE	5a. CONTRACT NUMBER
Flame Spread Along Free Edges of Thermally Thin Samples in Microgravity.	5b. GRANT NUMBER
	5c. PROGRAM ELEMENT NUMBER
6. AUTHOR(S)	5d. PROJECT NUMBER
	5e. TASK NUMBER
	5f. WORK UNIT NUMBER
7. PERFORMING ORGANIZATION NAME(S) AND ADDRESS(ES) **Chemical and Fuels Engineering Department University of Utah Salt Lake City, UT 84112, USA**	8. PERFORMING ORGANIZATION REPORT NUMBER
9. SPONSORING/MONITORING AGENCY NAME(S) AND ADDRESS(ES)	10. SPONSOR/MONITOR'S ACRONYM(S)
	11. SPONSOR/MONITOR'S REPORT NUMBER(S)

12. DISTRIBUTION/AVAILABILITY STATEMENT
Approved for public release, distribution unlimited

13. SUPPLEMENTARY NOTES
See also ADM001790, Proceedings of the Combustion Institute, Volume 28. Held in Edinburgh, Scotland on 30 July-4 August 2000., The original document contains color images.

14. ABSTRACT

15. SUBJECT TERMS

16. SECURITY CLASSIFICATION OF:			17. LIMITATION OF ABSTRACT	18. NUMBER OF PAGES	19a. NAME OF RESPONSIBLE PERSON
a. REPORT	b. ABSTRACT	c. THIS PAGE			
unclassified	**unclassified**	**unclassified**	**UU**	**7**	

Standard Form 298 (Rev. 8-98)
Prescribed by ANSI Std Z39-18

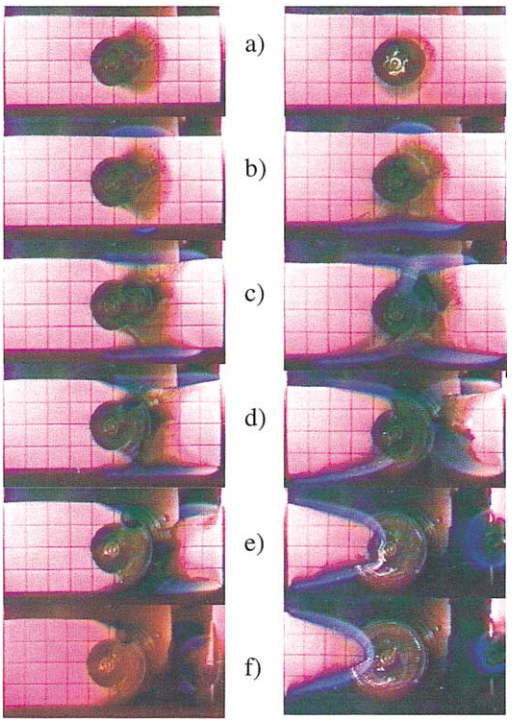

FIG. 1. Time sequence of images from two experiments (not constant time intervals): on the left is a 2 cm/s air flow test, and on the right is a 3.5 cm/s air flow test. Flow is from right to left. Sample width is 4 cm. Grid on sample surface is 1 cm square.

g/cm^2). The sample was installed in the center of the duct. The long edges of the sample were exposed to air. Ignition was initiated at the center of the sample instead of the edges, as shown in Fig. 1a, by radiation from a near-infrared tungsten/halogen lamp recessed in the duct wall. About a 1 cm circular area of the center part of the sample was blackened to enhance absorption of the incident radiation from the lamp. The radiant flux distribution was Gaussian with a peak flux of 10 kW/m^2 and a 1/e^2 (half width) radius of about 0.5 cm. Red light-emitting diodes were used to illuminate the sample surface so the dim blue flame could still be visible.

Experimental Results

As a part of the series of space experiments, four tests were conducted to examine the flame spread along free edges with slow external flows. Fig. 1 shows a sequence of video images from two of the tests. Ignition was initiated at the circular, blackened center, and transition to flame spread occurred in all directions except downstream. At the external flow velocities tested in this study, oxygen supply to the flame front was the rate controlling process, and downstream flame spread did not occur due to a lack of oxygen by virtue of its consumption by the upstream flame (oxygen shadow effect) [5]. In Fig. 1b, blue flame fronts reached both free edges of the sample. There were slight differences in the flame size between the upper and lower sample halves in the images because the time for the flame front to reach each free edge was slightly different. At 2 cm/s flow velocity, the flame did not spread appreciably downstream either along the free edges (edge flame spread) or the center part of the sample (central flame spread). The upstream flame fronts along the free edges were well ahead of that in the center part of the sample as seen from the concave char pattern shown in the left side of Fig. 1c–e. At 3.5 cm/s, however, flames did spread downstream along the free edges. Eventually, the upstream flame reached the end of the sample and became smaller (Fig. 1e–f). As the upstream flame shrank, decreasing its oxygen consumption, its oxygen shadow effect was reduced. This allowed the downstream edge flames to spread toward the center where they eventually met to form a continuous downstream spreading flame. This is consistent with the previously observed behavior of no downstream flame spread in the presence of upstream flame spread on samples without free edges in air velocities up to 6.5 cm/s [10].

The edge flame front positions in both upstream and downstream directions were tracked from the video images. When the flame front reached the free edges, a sudden, rapid flame spread occurred. However, the edge flame spread rates were reasonably steady after the initial acceleration in both upstream and downstream directions. The edge flame spread rates, determined from the slopes of the nearly straight-line part of the plots, are shown in Fig. 2 as a function of external air flow velocity. The upstream edge flame spread rate decreases slightly with an increase in external flow velocity. This trend is significantly different from that of the upstream central flame spread rate, which significantly increases with external flow velocity in this range of velocities. However, these edge flames are propagating much faster than a normal-gravity, downward, free-edge flame over the same sample, which propagates at approximately 0.13 cm/s against buoyancy-induced air flow. This suggests that edge flame spread rate would continue to decrease gradually with external flow velocity above 5 cm/s. However, downstream edge flame spread rate increases rapidly with an increase in external flow velocity.

To provide a perspective on edge flame spreading relative to central flame spreading, the edge flame spread rates were normalized by the central flame spread rates obtained from the samples without the free edges. The upstream and downstream central flame spread rates at each flow were used to normalize the upstream and downstream edge flame

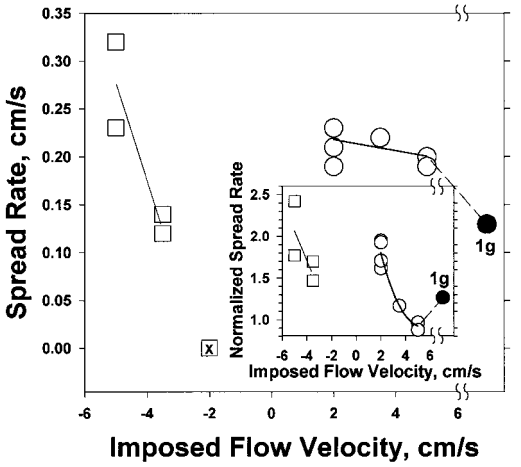

FIG. 2. The experimentally obtained relationship between edge flame spread rate and imposed flow velocity. Positive imposed flow velocity indicates the opposed flow condition and, therefore, an upstream flame spread configuration; negative imposed flow velocity indicates the downstream flame spread (concurrent flow condition). Solid circles are in a 1g environment. The symbol X means no spread. The insert is normalized edge flame spread rate by central flame spread rate for downstream and upstream directions, respectively.

spread rates at the corresponding flow velocity, respectively. The normal gravity downward edge flame spread rate was also normalized by the normal gravity downward central flame spread rate. As seen in the insert of Fig. 2, at low velocities the upstream edge flames spread faster than the upstream central flame. However, as imposed flow velocity increases, the oxygen supply to the central flame becomes sufficient and the upstream central flame spreads at the same rate as the upstream edge flame. This would be a minimum normalized upstream edge flame spread rate, because at normal gravity the normalized downward spreading edge flames are again faster than the central downward propagating flame. The downstream normalized edge flame spread rate increases rapidly with imposed flow, due to enhancements in both oxygen supply and convective heating.

Theoretical Model

Since a more detailed description of the mathematical model has been given in Refs. [10,11], only a brief summary is given here. The gas phase was formulated with the conservation equations of mass, full Navier-Stokes form of the momentum (without gravity), energy, and species (fuel and oxygen) under the low Mach number limit. A global one-step reaction (fuel gas) + υ_{O_2} (oxygen) $\rightarrow$ product with an Arrhenius rate was used. The same values for the kinetic constants of the gas phase and the condensed phase have been used in our previous theoretical studies [5,10,12]. Ignition was initiated by an external radiant flux on the sample surface. The sample was assumed to be thermally thin, and radiative heat losses from the surface were included. However, radiative heat transfer from flame to the sample was not significant for thermally thin samples [7], and also, the color of edge flames shown in Fig. 1 was blue. Therefore, radiative transfer from flame was not included.

There were two assumed symmetry planes. One was parallel to the plane of the sample passing through its center; the other was perpendicular to the plane of the sample, passing through the sample centerline parallel to its long axis. Thus, the three-dimensional simulation code [5,12] solved the conservation equations for flame spread along half a 4 cm by 10 cm sample enclosed in a 13 cm long $\times$ 4 cm wide $\times$ 5 cm tall rectangular computational volume. About 400,000 grid points (192 $\times$ 64 $\times$ 32) were used in the calculation. Cell sizes were 0.66 mm parallel to the sample and were increased from 0.25 mm at the sample surface to 2 mm at the top of the computational domain.

Theoretical Results

The calculation indicated that ignition was observed with air, but subsequent flame spread from the localized ignition was not attained with the kinetic constants and the material properties described above. However, the objective of the study was not necessarily to duplicate experimental results exactly by manipulating the model parameters, but rather to deduce trends of the phenomena. Therefore, calculations were made at higher oxygen concentrations of 29% and 33%. The calculated sequences of the flame images, similar to the experimental one shown in Fig. 1, are shown in Fig. 3. The bottom half of each sequence is a plot of the isosurface of the gas-phase reaction rate (5×10^{-5} g/cm^{3}s), which is chosen to represent a flame shape. The upper half of each sequence is fuel concentration at one grid cell above the sample surface (at 0.28 mm); the arrows in the bottom half are oxygen mass flux vectors. Here, discussion focuses on the flame shape; fuel and oxygen fields are discussed later. Shortly after ignition, the flame is more or less circular and is slightly extended upstream (Fig. 3a) as in the experimental case of Fig. 1a. Later, the flame spreads to both open edges (Fig. 3b) and starts to spread both upstream and downstream, but still as one continuous flame. For the case of 29% oxygen, the size of the downstream flame along the open edge is relatively small due to less oxygen supply (note length of oxygen mass flux vectors). At later

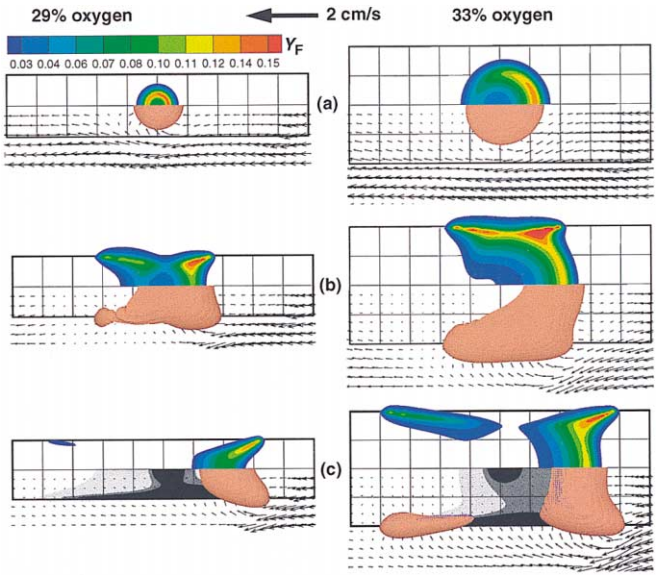

FIG. 3. Two calculated sequence images of fuel mass fraction (upper half of each sequence) and isosurface of gas-phase reaction rate (5×10^{-5} g/cm^{3}s) with net oxygen mass flux vectors (lower half of each sequence) at an imposed flow velocity of 2 cm/s. Fig. 3c includes the calculated char fraction contours of the sample in the lower half of both sequences. The sequence of 29% oxygen concentration is calculated with a 2 cm wide sample compared to a 4 cm wide sample in 33% oxygen concentration. The time sequence is at (a) 2.5 s, (b) 6 s, and (c) 10 s for the 29% oxygen and is at 5 s, 8 s, and 11 s for 33% oxygen. Flow is from right to left. Grid lines are 1 cm spaced.

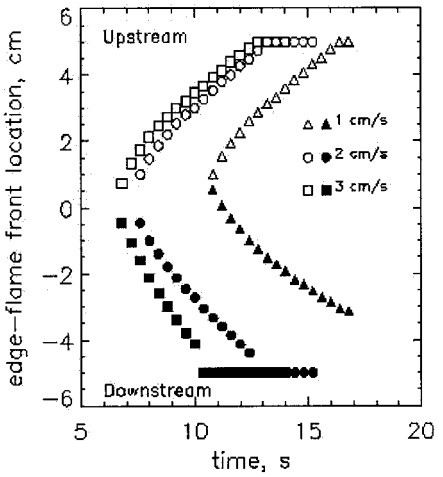

FIG. 4. The calculated relation between downstream and upstream edge flamefront locations in 33% oxygen concentration at various imposed velocities. Localized ignition is initiated at 0 cm.

times (Fig. 3c), in 33% oxygen concentration, the flame separates into three different zones; one spreads upstream and two separate flames spread downstream along open edges. The upstream flame spreads faster along open edges than over the center part. However, in 29% oxygen concentration, the downstream flame does not propagate either along the open edges or the center part. Overall trends shown in Fig. 3 are very similar to those shown in Fig. 1d.

The calculated results of the edge flamefront location with respect to time from the beginning of external radiation in 33% oxygen concentration are shown in Fig. 4. The plots are qualitatively very similar to the experimental data. The edge flame spread starts earlier as the imposed flow velocity increases due to faster lateral flame spread to the edges. Also, the starting locations of the edge flames shift upstream with decreasing imposed flow velocity. An initial acceleration in the edge flame spread occurs, followed by a nearly steady (linear) spread for 2 cm/s and 3 cm/s imposed flows. For 1 cm/s imposed flow, the downstream edge flame spread rate did not reach a steady state with the sample size used in this study. For longer samples, it is possible that this flame might extinguish. The steady edge flame spread rate is determined by the slope of the nearly linear part of the curves in Fig. 4, and also from a similar plot for 29% oxygen concentration (not shown). The results are plotted with respect to the imposed flow velocity in Fig. 5. This figure shows the same trends as observed in the experiments in Fig. 2; downstream edge flame spread rate increases rapidly with an increase in the imposed flow velocity, but the upstream edge flame spread rate is nearly independent or decreases slightly with the imposed flow velocity in the range used in this study.

Discussion

The spread rate of the upstream edge flame was greater than the upstream center flame due to improved oxygen supply along edges and also heat transfer from flame to the virgin sample surface. This

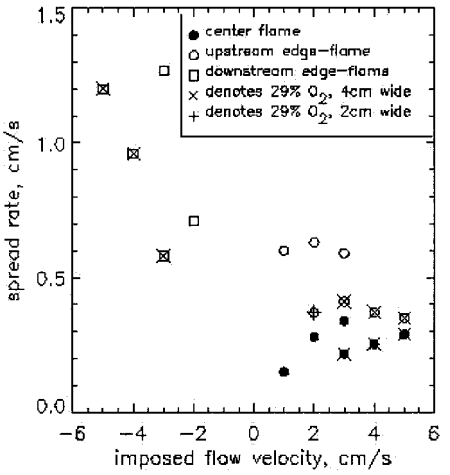

FIG. 5. The calculated spread rate with respect to imposed flow velocity in 29% (X on the symbol) and 33% oxygen concentrations. Open symbol is along an open edge, and solid symbol is over the center part of the sample.

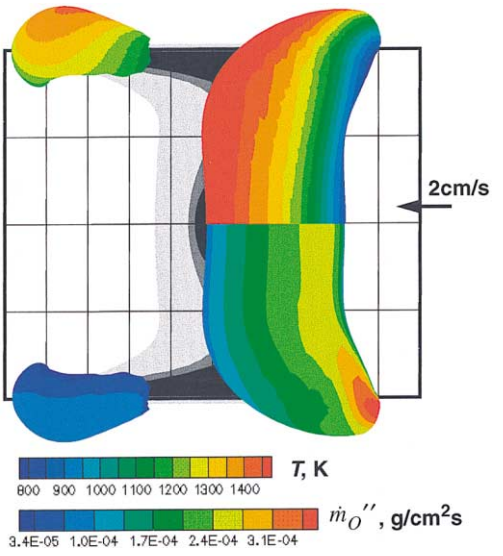

FIG. 6. On the bottom half are color contours of net oxygen mass flux normal to the 5×10^{-5} (g/cm^{3}s) reaction rate isosurface. On the top half is the same reaction rate isosurface colored by temperature (K). Char fraction contours of the sample are plotted in both halves. Conditions are in 33% oxygen concentration with 2 cm/s imposed flow at 11 s from irradiation. Flow is from right to left. Grid lines are 1 cm spaced.

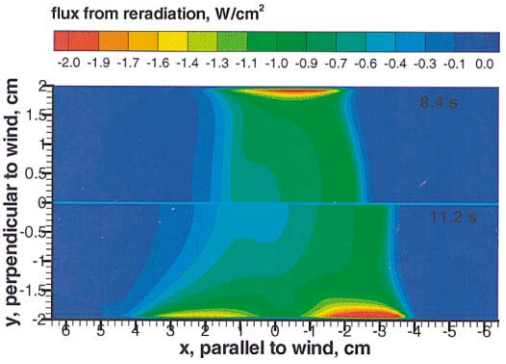

FIG. 7. The calculated distribution of heat feedback rate to the sample in 33% oxygen. The upper half is the imposed flow velocity of 3 cm/s and the lower half is 1 cm/s. The flow is from right to left. Ignition is initiated at $x = 0$ cm.

was particularly so at low imposed flow velocities because the diffusion process dominated over convection and the diffusion process was most enhanced at the open edges. The oxygen mass flux vectors clearly show this in Fig. 3. Also, the lower half of Fig. 6 shows that the amount of oxygen mass flux to the upstream edge flames is roughly two times higher than that to the central flame. Furthermore, heat transfer from flame to the sample surface is more efficient for edge flames than center flame due to geometrical edge flame shape with respect to the sample edge (roughly factor of 3 at 1 cm/s imposed flow) as shown in Fig. 7. (This enhancement in flux includes two effects; one is higher edge flame temperature due to larger oxygen supply to the flame and also increased heat transfer rate.) Note that the upstream edge flame spread rate is nearly independent of, or decreases slightly with, imposed flow velocity, compared with rapid increase for center flame. The calculated gas-phase temperature of the upstream edge flame, as shown in Fig. 6, does not increase with the flow velocity. This indicates that there is a sufficient oxygen supply to the edge flame, and further increase in the velocity will gradually cool the flame. Consequently, the heat flux from edge flame to the sample surface is nearly the same for two different imposed velocities as seen in Fig. 7. However, higher imposed flow velocity increases center flame temperature due to increased oxygen supply, and the heat flux from the center flame to the sample surface increases significantly as seen in Fig. 7. Oxygen supply to the downstream edge flames greatly exceeds that to the center part of the downstream flame spread, as shown in Figs. 3 and 6. Because the supply continues to increase with the imposed flow velocity, the downstream edge flame spread rate increases significantly with the imposed flow velocity.

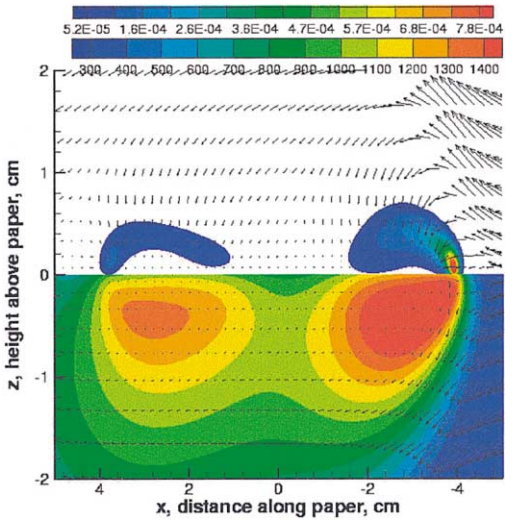

FIG. 8. The calculated gas-phase reaction rate distribution and gas-phase temperature distribution in a vertical plane along the open edge of the sample (the sample plane is at $z = 0$ cm). Conditions are 33% oxygen, time is 11 s, and 2 cm/s imposed flow velocity. Upper half of figure has color contours of gas-phase reaction rate and net oxygen mass flux vectors (convection + diffusion), and lower half has temperature color contours and convective oxygen mass flux vectors. Flow is from right to left. Ignition is initiated at $x = 0$ cm.

The next question is why the flame separated into upstream flame and downstream flame/flames as observed in the experiment and also in the calculation. When an upstream flame is present, the downstream flame can fail to spread because the upstream flame consumes too much oxygen, although heat feedback rate to the sample surface is sufficient [5,10,12]. This can be seen in Figs. 3, 6, and 7. When the imposed flow velocity is reduced, oxygen supply to the downstream flame becomes less, but still a sufficient amount of oxygen can be supplied to the downstream edge flames from the outer free stream mainly by diffusion. This is seen in Figs. 6 and 8. In Fig. 8, the difference between the total oxygen mass flux vector (upper plot) and convective oxygen mass flux vector (lower plot) is the oxygen supply flux vector to the flames by diffusion. The convective oxygen mass flux to the downstream edge flame is very small, as shown in the figure. Although the oxygen supply by diffusion to the flame continues along the downstream open edges, the fuel supply from the thermally thin sample (Fig. 3b) eventually becomes depleted. This causes the middle part of the edge flame to extinguish. The flame then separates into an upwind spreading flame across the entire sample and two downwind edge flames. If sufficient oxygen is present, the downwind edge flame survives (33% oxygen case); otherwise, it extinguishes (29% oxygen case).

Conclusion

The edge flame gets a greater oxygen supply from the outer free stream by convection and diffusion and has a more efficient heat transfer rate to the sample, due to the unique geometrical flame shape. Thus, flame spread along the open edges of a thermally thin cellulosic sample is faster than over its center part with an imposed flow velocity up to about 5 cm/s in microgravity. However, the upstream edge flame spread rate is nearly independent of or decreases gradually with the imposed flow velocity. When the imposed flow velocity is as low as 2 cm/s or less in air, downstream edge flame spread does not occur in the presence of the upstream flame, due to a lack of oxygen supply to the flame. However, downstream edge flame spread increases significantly with an increase in the imposed flow velocity. The transition from localized ignition to subsequent flame spread tends to occur along open edges at an imposed flow velocity which is lower than that required in the center area. Also, the edge flame tends to spread faster than the central flame. Therefore, flame spread along an open edge presented a greater fire hazard in microgravity in the range of the imposed flow velocity used in this study, and three-dimensional modeling is critically needed to describe realistic fire phenomena.

Acknowledgments

This work is funded by the NASA Microgravity Science Program under the Inter-Agency Agreement No. C-32001-R under technical monitoring of Dr. Sandra Olson.

REFERENCES

1. Olson, S. L., *Combust. Sci. Technol.* 76:233–249 (1991).
2. Grayson, G. D., Sacksteder, K., Ferkul, P. V. and T'ien, J. S., *Micrograv. Sci. Technol.* 99:345–370 (1994).
3. Bhattacharjee, S., Altenkirch, R. A., and Sacksteder, K., *J. Heat Transfer* 118:181–190 (1996).
4. Bhattacharjee, S., Altenkirch, R. A., and Sacksteder, K., *Combust. Sci. Technol.* 91:225–242 (1993).
5. Kashiwagi, T., McGrattan, K. B., Olson, S. L., Fujita, O., Kikuchi, M., and Ito, K., *Proc. Combust. Inst.* 26:1345–1352 (1996).
6. West, J., Tang, L., Altenkirch, R. A., Bhattacharjee, S., Sacksteder, K., and Delichatsios, M. A., *Proc. Combust. Inst.* 26:1335–1343 (1996).

7. Altenkirch, R. A., Tang, L., Sacksteder, K., Bhattacharjee, S., and Delichatsios, M. A., *Proc. Combust. Inst.* 27:2515–2524 (1998).
8. Emmons, H. W., and Shen, T., *Proc. Combust. Inst.* 13:917–926 (1971).
9. Markstein, G. H., and de Ris, J., *J. Fire Flamm.* 6:140–154 (1975).
10. McGrattan, K. B., Kashiwagi, T., Baum, H. R., and Olson, S. L., *Combust. Flame* 106:377–391 (1996).
11. Nakabe, K., McGrattan, K. B., Kashiwagi, T., Baum, H. R., Yamashita, H., and Kushida, G., *Combust. Flame* 98:361–374 (1994).
12. Mell, W. E., and Kashiwagi, T., *Proc. Combust. Inst.* 27:2635–2641 (1998).

COMMENTS

Carlos Fernadez-Pello, University of California Berkeley, USA. That the flame spread faster on the edges is also observed with thick fuels in normal quantity. Do you think in that case oxygen supply is the reason for the faster spread rate or is it also enhancement of heat transfer to the solid?

Author's Reply. In normal gravity, buoyancy-induced flow velocity is much higher than the velocity range used in this study, the supply of oxygen to flame front is sufficient, and heat transfer from flame to the sample surface ahead of the flame is the rate-controlling step. Therefore, enhancement of heat transfer is the reason for faster flame spread rate over free edges or open corners.

•

John L. de Ris, Factory Mutual Research, USA. A very interesting paper. It appears from your photographs that the flame stand-off distance from the edge is considerably greater in the experiment than predicted from the model. If this is the case, could you please comment on the reason?

Author's Reply. The flame picture you are referring to, which I showed in the early part of the presentation, was not for the case of flame spread along open edges but was for flame spread along the center of the sample. This picture was used to show that flame spread occurs only in the upstream direction when the sample is ignited locally (spot ignition) in the center of the sample. The model predictions you refer to were in vertical planes along the open edge of the sample. However, it is nearly impossible to experimentally observe the flame stand-off distance for spread along open edges because the flame entirely surrounds the open edge. We therefore used side-view flame pictures taken in the two-dimensional configuration (nearly line-shape flame across the sample) to estimate the flame stand-off. The experiment was conducted in a 10 s drop tower in 35% oxygen concentration under 2 cm/s wind using a 10 cm wide sample. The experimentally determined cross section of the flame is compared with that calculated by our two-dimensional code with the same wind and oxygen conditions. The simulated flame shape is determined by the gas-phase reaction rate distribution; note that the shape will depend on the selection of the gas-phase reaction rate. The simulation flame stand-off distance at the flame tip (about 3.5 mm at highest reaction rate) is very close to the measured values based the tip of the yellowish flame (about 3.7 mm). However, the blue color part of the flame is ahead of the yellowish flame front and is very close to the sample surface (it is difficult to determine but appears to be roughly 1 mm) and the calculated gas-phase reaction rate extends close to the sample surface.